First Order Ether Drift Experiment

Ling Jun Wang

Department of Physics, Geology and Astronomy, University of Tennessee at Chattanooga

Chattanooga, TN 37403; lingjun-wang@utc.edu

Published in *Physics Essays*, Vol. 23 No. 3（2010)

Keywords: ether drift experiment, experimental relativity, null result.
Des Mots clés: une expérience de la dérive d'éther, la relativité expérimentale, un résultat nul

Abstract

We have carried out a first order ether drift experiment over a period of two years. The signal to noise ratio of our first order experiment is four orders of magnitude greater than that of the second order experiments. The rotational velocity and the orbital velocity of the earth, and the galactic orbital velocity of the solar system with respect to the ether have been measured to be, respectively, 0.051 *km/s*, -0.19 *km/s* and 0.30 *km/s*, with a statistical error of 0.94 *km/s*. These velocities are merely 14%, 0.6% and 0.15% of the kinetic velocities of the earth and the solar system with respect to the Milky Way. The results show that the ether drift velocity with respect to the earth is zero well within experimental uncertainty. Since this uncertainty is greater than the velocity due to Earth's rotation, the experimental error needs to be further reduced to establish the "null result" with respect to Earth's rotation beyond doubt.

Our experiment is fundamentally different in principle from the traditional ether drift experiments based on the interference of light. In particular, our experiment is free of the fringe running problems during the rotation of the interferometer, and therefore contributes a truly independent experiment from the interference experiments.

Un Abrégé

Nous avons réalisé une expérience de la dérive d'éther de premier ordre sur une période de deux ans. Le rapport signal - bruit de notre expérience de premier ordre est de quatre ordres de magnitude plus grand que l'expérimentation de deuxième ordre. La vitesse de rotation et la vitesse orbitale de la terre, et la vitesse orbitale galactique du système solaire par rapport `a l'éther ont été mesurées à être, respectivement, 0.051 *km/s*, -0.19 *km/s* and 0.30 *km/s*, avec une erreur statistique de 0.94 *km/s*. Ces vitesses sont simplement 14%, 0.6% et 0.15% des vitesses cinétiques de la terre et du système solaire `a l'égard de la Voie Lactée. Les résultats montrent que la vitesse de la dérive d'éther par rapport à la terre est zéro bien dans les limites de l'incertitude expérimentale. Puisque cette incertitude est plus grande que la vitesse `a cause de la rotation de la Terre, l'erreur expérimentale doit être réduite davantage pour établir "le résultat nul" par rapport `a la rotation de la Terre sans aucun doute.

Notre expérience est fondamentalement différente en principe des expériences traditionnelles de la dérive d'éther basées sur l'interférence de la lumière. En particulier, notre expérience est libre de la frange des problèmes en cours d'exécution lors de la rotation de

l’interféromètre, et contribue donc une expérience véritablement indépendante des expériences d’interférence.

1. Historical Background

The historical ether drift experiment by Michelson and Morley [1,2] played a fundamental role in the development of the theory of relativity, and is the single most important macroscopic experiment that offered pillar support to Einstein's theory. It can be said that the null result of the ether drift experiment was largely responsible for the public acceptance of relativity when the indirect evidences of microscopic experiments were not yet available.

In designing the ether drift experiment, Michelson was originally hoping to have a first order experiment, i.e., the fringe shift was to be linearly proportional to (v/c), where v and c were respectively the drift velocity and the speed of light. However, the experiment turned out to be a one of second order, i.e., the fringe shift was proportional to $(v/c)^2$. Since (v/c) was about 10^{-4}, the signal-to-noise ratios of the first and the second order experiments would differ by about 4 orders of magnitude. Such extremely small signal-to-noise ratio explained much of the challenges facing the Michelson-Morley experiment and its later variations. The interference fringes were expected to shift by about 0.3 fringes if the interferometer rotated by 90^o. Such signal was extremely small against the various huge noises due to extremely high sensitivity of the Michelson interferometer, which was so sensitive that it could pick up the motion of the vehicles and pedestrians on the streets outside the campus of Case-Western Reserve University.

The problem with the extremely low signal-to-noise ratio generated a more serious and fundamental problem of fringe running during the rotation of the interferometer. Since the Michelson interferometer could pick up noises of the mechanical vibration of the interferometer and the operators who pushed it rotating, the noises could cause the interference fringes to run by much more than the fringe shift due to genuine ether drift. The interference fringes would run back and forth with high speed through the viewing field. Since such fringe running was merely a running of the interference pattern without involving physical movement of any object, the running speed of fringes was theoretically allowed to be greater than the speed of light. Practically, the fringe running during the rotation is too fast to be followed and recorded by any instrument, let alone human eyes. The fringe running was actually more serious a problem than the noise itself. Suppose, after the interferometer came to a complete stop after rotating for 90^o, the signal and the noise together caused the interference pattern to shift by 4.2 fringes, it will be recorded as 0.2 instead of 4.2, and 1.9 would be recorded as -0.1 and so on, due to the fact that there was no way to keep track of the fringe running during the rotation of the interferometer. Namely, one could only record the difference between the signal and the nearest integer instead of the true fringe shift itself. Such difference ought to be random in nature and will be averaged to zero by statistics. It constituted a fundamental doubt in the credibility of the null result from experimentalist point of view.

Another concern about the null result of Michelson-Morley experiment was the possibility of chance cancellation of the spinning speed of the earth and the orbiting speed of the earth about the sun by that of the solar system about the galactic center. To eliminate such uncertainty, it was necessary to repeat the measurement in the different seasons of an entire year. Einstein therefore encouraged Michelson to repeat his ether drift experiment to address the issue. Although Michelson did repeat the experiment up in Mt. Wilson, he was, however, never able to carry out the experiment over a period of whole year.

Michelson's experiment was repeated with modifications by many researchers [3]. The repetitions of Michelson's experiment were all second order experiments. These repetitions eliminated the possibility of chance cancellation, but failed to address the fringe-running issue. In principle, any experiment based on measurement of fringe shift is prone to the fringe running problem, which was not addressed anywhere to the best of our knowledge.

The theory of relativity has been built into the foundation of modern physics. There seems to be little room for doubt or need for repetition of the ether drift experiment. The challenges, however, do exist. Ole Roemer, a Danish astronomer, has observed that Io, the innermost satellite of Jupiter, undergoes a regular variation in its period of revolution as the Earth revolves around the Sun. This is known as the Roemer Effect and can be classically explained by the Galilean velocity addition of the orbiting velocity of the earth to the speed of light. Namely, to the observer on Earth, the speed of light is not constant, but is equal to the vector addition of the speed of light in vacuum and the kinetic velocity v of the Earth on which the observer is at rest, contradicting the relativistic Principle of constancy of the speed of light. The Roemer Effect is considered as a successful detection of the ether drift motion[4-6].

The relative motion of the earth with respect to the ether would cause Doppler shift of the spectral lines of the stars, which is also linearly proportional to the ratio of the orbiting velocity of the earth to the speed of light. Such Doppler effect has been confirmed to a high degree of accuracy and is routinely used to determine the speed of revolution of the Earth[7]. This Doppler effect is also considered a first order experiment that successfully detected the ether drift[6].

These first-order experiments are classified as the Type I experiments in which there is relative motion between the source and the detector. The Michelson interferometer experiments and its later varieties are the Type II experiments in which there is no relative motion between the source and the detector. Mascart summarized the results of all the ether drift experiments know to him and his own experiments in which a static water tank was inserted in one of the two arms of the interferometer[8]. He concluded that all Type II experiments were incapable of detecting the motion of the Earth relative to the ether. Veltmann and Potier [8] provided theoretical justification for Mascart's conclusion by combining Fresnel's theory with Fermat's principle of least time. They have shown that Snell's law (and therefore the index of refraction) is the same for stationary or moving media and the interference phenomena are independent of the state of motion of the medium. They have established a so-called Potier-Veltmann principle which stgates that the absolute motion of the Earth with respect to the ether is undetectable to the first order in v/c. Namely, only the second-order effect of the ether drift can be detected if an interferometer is used in such Type II experiment. Mascart was unable to repeat Fizeau's result, nor could any one elso[8]. It was generally accepted that an experimental flaw (perhaps a temperature gradient) had caused the results.

Cahill [9-12] has recently reinterpreted the Michelson-Morley experiments and claimed that a different calibration based on the Fitzgerald-Lorentz contraction effect would lead to a positive ether drift effect with a speed greater than 300 km/s of the Earth. Cahill's work was basically a theoretical reinterpretation based on Fitzgerald-Lorentz contraction instead of Einstein's theory of relativity. Whether or not the Fitzgerald-Lorentz contraction is a more suitable theory than Einstein's theory of relativity is quite debatable an issue, as far as the interpretation of Michelson's

experiment is concerned, the two theories are basically equivalent. But Cahill did give a good account of the experiments that had shown the positive ether drift effect. Miller's interferometer experiment at Mt. Wilson in 1925/26 showed the absolute motion of the Earth[13]. DeWitte's measurements of the one-way travel time of Radio Frequency EM waves in coaxial cable, and Torr and Kolen's similar measurements of the EM waves all showed the absolute motion[14]. It should be noted that all these results were obtained in gas-filled coaxial cables. Analogous optical fiber experiments and the transparent solids in a Michelson interferometer all give null results. It shows that the Fizeau's ether drag effect does not apply in the solid media. It also suggests that the results of the experiments enclosed by transparent or non transparent solids, such as the one carried out in basements or in vacuum, are dubious.

From experimental point of view, an independent macroscopic first order experiment based on completely different principle from that of the Michelson interference experiment would undoubtedly help to settle experimental foundation for theoretical work when there are serious doubts about the original experiments. We have designed and carried out a first order ether drift experiment that is immune of the fringe running problem because it does not involve interference. It is a Type II experiment because there is no relative motion between the source and the detector. It is a first order experiment because the light path takes a one-way trip. The signal to noise ratio of this experiment is theoretically four orders of magnitude better than the historical second order experiments. The theory and the experimental design are amazingly simple as compared to the second order experiments.

2. Experimental Set-up

The experimental design is shown in Figure 1. An 18 feet long steel pipe with a diameter of 15" and thickness of 1.5" is mounted on a houseboat floating on a circular pond. The weight of the steel pipe is estimated to be 1.5 tons as calculated from its measurements, and the total weight of the steel pipe and the houseboat is estimated to be 3 tons from the measurements of the boat and the draft. One end of the house boat is pivoted at the center of the pond to allow rotational movement. A diode Laser is mounted on the end of the steel pipe near the center of the pond. The laser beam is sent to a linear array detector mounted on the opposite end of the steel pipe. The linear array is mounted perpendicular to the axis of the steel pipe to detect the deviation of the laser beam from the axis caused by possible ether drift. A photograph of the experimental set-up is shown in Figure 9.

As shown in Figure 2, the arrowed line OO' is the laser beam. If the velocity of the earth is aligned with the laser beam, it will hit the point O' on the linear array detector. If, however, the earth is moving in the ether with velocity V that is making an angle of θ with the laser beam, the point O' of the linear array detector would have moved to the point O" by the time the laser beam hits the array, and it will hit the point x on the linear array away from the point O". The amount of shift can be easily calculated to be

$$x = Vt \sin\theta$$

where L' is the light path of the laser beam, the distance between points O and O". V and c are, respectively, the drift velocity of the earth with respect to ether and the speed of light. Let the length of the steel pipe be L, we have

$$L' = ct = L + Vt\cos\theta$$
$$t = \frac{L}{c - V\cos\theta} \approx \frac{L}{c}(1 + \frac{V}{c}\cos\theta)$$
$$x = Vt\sin\theta = \frac{LV}{c}\sin\theta(1 + \frac{V}{c}\cos\theta)$$
$$= \frac{LV\sin\theta}{c} + L\sin\theta\cos\theta\frac{V^2}{c^2}$$
$$\approx \frac{LV\sin\theta}{c}$$

We have ignored the second term because it is a second order effect. We therefore have:

$$x = Vt\sin\theta = \frac{LV}{c}\sin\theta \qquad (1)$$

It should be noted that this shift of the laser beam position on the linear array detector has no fringe running problem, which is intrinsic to the interference experiments. Equation (1) shows that the shift of laser position on the linear array is a sinusoidal function of the orientation angle of the laser beam when the experimental set up is allowed to rotate about the center of the circular pond.

We can estimate the expected signal if the earth is moving relative to the optical medium (ether) and the said medium is at rest relative to the galaxies. The length L is 5.5 meters and the velocity of the earth with respect to the sun is about 30 km/s. This would give a peak shift of about 0.55 mm. This shift can be easily detected with a linear array, which has an array length of 8 mm and a pixel size of 7.8 μm. We therefore expect the amplitude of the sinusoidal function in Eq.1 to be about 70 pixels if the optical medium is at rest with the galaxies.

3. Theoretical calculation

The relative velocity of the experimental set-up with respect to the ether is a composite function of the spinning angular velocity of the earth, the orbiting velocity of the earth around the sun and the velocity of the solar system orbiting the galactic center. In this section we will calculate these velocities as measured at the site of experiment in Chattanooga, Tennessee of The United States.

3.1. The velocity due to rotation of the earth

The sidereal rotation period of the earth is 23 hours 56 minutes 4.1 seconds, which is 23.93447 hours, or 86164.1 seconds. The radius R of the earth is 6378 km. The site of experimental set up, Chattanooga, Tennessee of USA, has a latitude of 35°11' = 35.18° and a longitude of 85.0195°. The distance from the site to the rotational axis of the earth is

$$r = R\cos 35.18^o = 5213km \tag{2}$$

The linear velocity of the equipment due to the rotation of the earth is

$$v_s* = \frac{2\pi \times 5213km}{86164.1s} = 0.38014km/s \tag{3}$$

This velocity is always directed to the local east.

3.2 The orbiting velocity of earth around the sun

The sidereal year of the earth is 365.26 days. The distance from the earth to the sun is 1.496 x 10^8 km. The orbital velocity of the earth around the sun is

$$v_0* = 29.785km/s \tag{4}$$

The orbiting velocity is tangent to the local surface of the earth at noon or midnight, making an inclination angle α with the equator. But our experiments are not performed at midnight. To calculate the projection of the orbital velocity onto the axis of the local coordinate system at the time of experiment, we will do a two step transformation: 1) transformation of the orbital velocity from the coordinate system at the point A on the equator which is at midnight when the data is taken, to point B on the equator having the same longitude of Chattanooga; 2) transformation of the velocity from point B to the local system of Chattanooga. We choose east to be the *x*-direction, north the y-direction, and the local zenith the z-direction for all three points.

a) Transformation of the orbital velocity from point A to point B on the equator

As shown in Figure 3, the orbital velocity at point A at midnight is

$$\begin{cases} v_{Ax} = v_o \cos\alpha \\ v_{Ay} = v_o \sin\alpha \\ v_{Az} = 0 \end{cases} \tag{5}$$

where α is the angle of inclination:

$$\begin{aligned} &\alpha = 23.5^o \sin\beta = 0.41015\sin\beta \\ &\beta = \Omega T \\ &\Omega = \frac{2\pi}{365.26} \text{ radians} \end{aligned} \tag{6}$$

where Ω is the angular velocity of the earth orbiting the sun, and T the time in days measured from the Summer solstice (June 22). v_o is the orbital velocity with respect to the ether, which has to be determined from the experimental data to be compared to the theoretical value v_o^* given by Eq.(4).

Translated to point B, as shown in Figure 4, the velocity is

$$\begin{cases} v_{Bx} = v_{Ax}\cos\phi = v_o\cos\alpha\cos\phi = -v_o\cos\alpha\cos\gamma \\ v_{By} = v_{Ay} = v_o\sin\alpha \\ v_{Bz} = -v_{Ax}\sin\phi = -v_o\cos\alpha\sin\phi = -v_o\cos\alpha\sin\gamma \end{cases} \quad (7)$$

with
$$\begin{cases} \gamma = \omega t \\ \omega = \dfrac{\pi}{720} \\ \phi = \pi - \gamma \end{cases} \quad (8)$$

where ϕ is the longitudinal difference between points A and B measured in radians, and t is the time interval in minutes measured from the noon to the time of experiment. $\omega = \dfrac{\pi}{720}$ (radians per minute), which is the rotational angular velocity of the earth.

b) Transformation of the orbital velocity from point B to the local system O at Chattanooga

Referring to Figure 5, the orbital velocity translated to the local system O is given by

$$\begin{cases} v_{Ox} = v_{Bx} = -v_o\cos\alpha\cos\gamma \\ v_{Oy} = v_{By}\cos\theta - v_{Bz}\sin\theta = v_o\sin\alpha\cos\theta + v_o\cos\alpha\sin\theta\sin\gamma \end{cases} \quad (9)$$

where θ =35.18º is the latitude of Chattanooga. The Z-component of the velocity in the local system is not included in our consideration because there is no experimental data for comparison.

3.3 The orbital velocity of the solar system with respect to Chattanooga

The orbiting velocity of the solar system about the galactic center can be reasonably assumed to be constant in a time span of two years of data collection. This drift velocity would have different velocity components in the local coordinate system O depending on the time of the day and the time of the year. Let us consider the two points O and B on earth. Point O is at Chattanooga, the site of experiment, and point B is the point on the equator having the same longitude as that of point O. The velocity of the solar system with respect to the ether can be expressed as the components $v_{x0,}$ $v_{y0,}$ and v_{z0} in the B system at noon of the Summer solstice (June 22) of the year 2007. Since the Y axis of the B system is parallel to the axis of the earth, the Y-component of the velocity in the B coordinate system remains constant at all times. The X and Z components of the velocity, however, change according to the date of the year and the time of the day due to orbital and rotational movement of the earth, as shown in Figure 6:

$$\begin{cases} v_{x'} = v_{x0}\cos\delta - v_{z0}\sin\delta \\ v_{y'} = v_{y0} \\ v_{z'} = v_{x0}\sin\delta + v_{z0}\cos\delta \end{cases} \quad (10)$$

where $\delta = \beta + \gamma$ (11)

Translated to the system O, referring to Figure 5,

$$\begin{cases} v_x = v_{x'} = v_{x0}\cos\delta - v_{z0}\sin\delta \\ v_y = v_{y'}\cos\theta - v_{z'}\sin\theta = v_{y0}\cos\theta - v_{x0}\sin\delta\sin\theta - v_{z0}\cos\delta\sin\theta \end{cases} \quad (12)$$

Again we ignored the Z-component. Adding Eqs.(3), (9) and (12) together, we obtain the local resultant drift velocity of the experimental set-up to be

$$\begin{cases} v_E = v_s - v_0\cos\alpha\cos\gamma + v_{x0}\cos\delta - v_{z0}\sin\delta \\ v_N = v_0\sin\alpha\cos\theta + v_0\cos\alpha\sin\theta\sin\gamma + v_{y0}\cos\theta - v_{x0}\sin\theta\sin\delta - v_{z0}\sin\theta\cos\delta \end{cases} \quad (13)$$

where v_E and v_N are the components of the drift velocity in the east and the north directions at the site of experiment.

4. Experiment

4.1 The equipment

The two key devices of the experiment are the laser and the linear array detector. We employed a diode laser made by Strait-Line Company designed for alignment applications. The shift of the light beam in the horizontal direction is detected by the linear array. One shortcoming of this laser is that the built-in focusing element distorted the beam profile with irregular noise superposed on a Gaussian curve. Such noise turned out not to be much a problem when we fit the curve into a Gaussian. Figure 7 shows the laser beam profile and the Gaussian fit by a software KaleidaGraph published and distributed by Synergy Software. The correlation is about 0.997, and the standard deviation of the center position of the Gaussian curve is 0.24 channels, which corresponds to 1.7 μm. This Gaussian peak is used to calculate the shift of the laser beam position. Since the peak position is determined by fitting 1024 data points into a Gaussian curve, its accuracy is better than that of a single channel by a factor of 32 (square root of 1024). The laser has a power output less than 5 mW, and the wavelength is in the range of 630-660 nm as specified. The laser wavelength is not important in our experiment, because the shift of beam position, instead of the interference pattern, is detected directly by a linear array. The laser is mounted on a 2” angle iron which is in tern mounted on one end of the steel pipe. The orientation of the angle iron can be adjusted in both horizontal and vertical directions by threaded rods to align the laser beam with the linear array detector mounted on the opposite end of the steel pipe.

We have employed a linear array detector CMOS LARRY-USB 1024 manufactured by Ames Photonics Inc., which has a linear array of 1024 elements. Each element is 7.8 μm wide and 125 μm high. The total active length of the array is 8 mm. The detector is enclosed in a light-tight metal box with only a 2mm x 10 mm horizontal window facing the laser beam. The window is covered by a goggle glass which serves dual purpose of shielding the light pollution and reducing the beam intensity to the level most comfortable for the linear array. It also provides a weather proof protection for the detector. The base of the detector can be adjusted horizontally by a

micrometer, and be locked. The linear array detector is interfaced via a USB cable to a laptop computer IBM ThinkPad. The data acquisition is carried out by a software Spectra-Array developed by Ames Photonics Inc., which allows the user to set the average time, the number of scans for averaging, and other convenient settings for easy operation and display. For best results we set the integration time to be 1 ms with 16 scans for averaging. This set of settings allows us enough integration time and number of scans for averaging against noises, and reasonable data acquisition speed against long term drift of laser position due to the change of environmental temperature. The integration and averaging take about 16 seconds for each data point. The data is stored in text files for analysis by the software KaleidaGraph, which also plots the data, fits the data into a Gaussian curve, and calculates the position of the fitted Gaussian curve and the correlation factor.

4.2 Stability and zero check

The stability of the equipment is crucial to the accuracy of the results. As shown above, the expected signal is about 0.55 mm, or 70 pixels. Our goal is to keep the uncertainty much less than this level. To insure this, we have conducted the following stability tests and zero checks:

a) The dark current of the linear array.

The dark current of the linear array registers a maximum of 112 counts when the integration time is set to 1 ms. This dark current is added to the signal of the laser beam, but does not show any difference in the peak position of the Gaussian curve. We tried to fit the data into a Gaussian with and without subtracting the dark current. The positions of the Gaussian curves are identical to the last digit.

b) The environmental light pollution

To avoid the light pollution, the experiments are carried out after dark in the evenings. The light pollution is almost completely cut out by the goggle glass on the window of the detector box. The peak position shows no change at all when the curve is fitted into Gaussian with or without the background subtracted. But a background measurement is taken anyway at the beginning of every experiment simply for archiving purposes. The data show that the environmental light pollution adds nothing to the background counts of the dark current.

c) The mechanical stability

To check the mechanical stability of the set-up against the vibration disturbance of the environment, especially the wind and the water waves, we have purposely rocked the houseboat so that the water waves are much higher than the highest waves in the thunderstorms. No shift of laser beam is observed to be caused by such disturbance if the measurements are taken within a few minutes. To be on the save side, we conducted our experiments in the quiet evenings of sunny days without strong wind. Waiting for good calm weather was one of the reasons that the experiments were occasionally not performed exactly once a week. The other reason was my inconvenient travel schedule.

d) The temporal stability

The major source of instability comes from the temperature change during warm-up period. The temperature change can cause the direction of the laser beam to change, as it contains a built-in one dimensional focusing element. This slight change of beam direction would translate into considerable shift of laser position at the detector 5.5 meters away. Experimental tests have shown that laser position shift during the warm-up period reduces exponentially as a function of time. To reduce this temporal shift to reasonably low level, two measures have been taken: a) A two hour warm-up period is allowed for the system to stabilize before data taking; b) The data is collected first by rotating the houseboat counterclockwise as viewed from the top for a full circle, collecting data at 16 evenly spaced angular positions, and then rotating clockwise back to the original position, taking another set of 16 measurements at the same positions. The laser beam position on the linear array at certain angular position is taken as the average of the two measurements. The whole data taking process lasts about 40 minutes. The temporal drift during this time period is reduced to less than 3 pixels, or 24 μm.

4.3 The data collection

The houseboat is manually rotated to stop gently at each of the 16 evenly spaced angular positions that are 22.5° apart. Due to constructional convenience, the zero position is not exactly south of the center of rotation, but at 9° east of south. The houseboat is rotated counterclockwise as viewed from above to take a set of data at each of the 16 positions, and then rotated clockwise back to the starting position, taking a set of data again at each position. The whole measurement takes about 40 minutes. The two sets of data at each position are averaged to minimize the temporal drift of the laser beam position due to temperature change.

The shift is a sinusoidal function of the orientation angle of the laser beam. We therefore fit the shift into a sinusoidal function:

$$S = a + b\theta + c\sin(\theta + \theta_0) \tag{14}$$

where S is the shift of the laser beam position. The first term in Eq(14) is a constant dependent on the arbitrary initial laser position on the linear array. It has no significance in our measurements. The second term is the temporal shift due to change of the environmental temperature. To reduce this temporal shift to an acceptable level, the equipment is turned on for two hours before data taking so that the laser and the whole set-up are thermally stabilized. The long warm-up time reduced the temporal shift enough to justify a linear representation. From the amplitude c and the initial phase angle θ_0 we obtain the X and Y components, v_{Ei}^* and v_{Ni}^*, of the resultant drift velocity. One set of data is taken every week, usually in the weekends if weather and the travel schedule permit. 90 sets of data have been taken over a period of two years, from April 28, 2007 to May 2, 2009. Figure 8 shows a representative set of data and the fitting it into Eq(14).

4.4 The Daylight Saving Time

The one hour Daylight Saving Time change in America is adjusted back to regular time in the time record. The Daylight Saving Time started from March 11 to November 4 in 2007, from March 9 to November 2 in 2008, and from March 8 to November 1 in 2009.

5. Data Analysis

Eq(13) contains five parameters: v_s, v_o, v_{xo}, v_{yo} and v_{zo}. These parameters are determined by fitting the experimental data into Eq(13) with the requirement that the root mean square error

$$\sigma = \sqrt{\frac{\sum_i [(v_{Ei} - v_{Ei}^*)^2 + (v_{Ni} - v_{Ni}^*)^2}{N-1}} \tag{15}$$

reaches the minimum, where v_{Ei} and v_{Ni} are given by Eq(13) while v_{Ei}^* and v_{Ni}^* are determined from the experimental data as described in section 4.3.

We therefore have

$$\begin{cases} \dfrac{\partial \sigma}{\partial v_s} = 0 \\ \dfrac{\partial \sigma}{\partial v_0} = 0 \\ \dfrac{\partial \sigma}{\partial v_{x0}} = 0 \\ \dfrac{\partial \sigma}{\partial v_{y0}} = 0 \\ \dfrac{\partial \sigma}{\partial v_{z0}} = 0 \end{cases} \tag{16}$$

which leads to

$$\begin{cases} a_{11}v_s + a_{12}v_0 + a_{13}v_{x0} + a_{14}v_{y0} + a_{15}v_{z0} = b_1 \\ a_{21}v_s + a_{22}v_0 + a_{23}v_{x0} + a_{24}v_{y0} + a_{25}v_{z0} = b_2 \\ a_{31}v_s + a_{32}v_0 + a_{33}v_{x0} + a_{34}v_{y0} + a_{35}v_{z0} = b_3 \\ a_{41}v_s + a_{42}v_0 + a_{43}v_{x0} + a_{44}v_{y0} + a_{45}v_{z0} = b_4 \\ a_{51}v_s + a_{52}v_0 + a_{53}v_{x0} + a_{54}v_{y0} + a_{55}v_{z0} = b_5 \end{cases} \tag{17}$$

with

$$a_{11} = N \tag{18.1}$$

$$a_{12} = a_{21} = -\sum_i^N \cos\alpha_i \cos\gamma_i \tag{18.2}$$

$$a_{13} = a_{31} = \sum_i^N \cos\delta_i \tag{18.3}$$

$$a_{14} = a_{41} = 0 \tag{18.4}$$

$$a_{15} = a_{51} = -\sum_i^N \sin\delta_i \tag{18.5}$$

$$a_{22} = \sum_i^N [(\cos\alpha_i \cos\gamma_i)^2 + (\cos\theta \sin\alpha_i + \sin\theta \cos\alpha_i \sin\gamma_i)^2] \tag{18.6}$$

$$a_{23} = -\sum_i^N \cos\alpha_i \cos\delta_i \cos\gamma_i - \sin\theta\cos\theta \sum \sin\alpha_i \sin\delta_i - \sin^2\theta \sum_i^N \cos\alpha_i \sin\delta_i \sin\gamma_i \tag{18.7}$$

$$a_{24} = a_{42} = \cos^2\theta \sum_i^N \sin\alpha_i + \frac{1}{2}\sin(2\theta)\sum \cos\alpha_i \sin\gamma_i \tag{18.8}$$

$$a_{25} = a_{52} = \sum_i^N \cos\alpha_i \sin\delta_i \cos\gamma_i - \frac{1}{2}\sin(2\theta)\sum_i^N \sin\alpha_i \cos\delta_i - \sin^2\theta \sum_i^N \cos\alpha_i \cos\delta_i \sin\gamma_i \tag{18.9}$$

$$a_{32} = a_{23} \tag{18.10}$$

$$a_{33} = N - \cos^2\theta \sum_i^N \sin^2\delta_i \tag{18.11}$$

$$a_{34} = a_{43} = -\frac{1}{2}\sin(2\theta)\sum_i^N \sin\delta_i = \frac{1}{2}\sin(2\theta) a_{15} \tag{18.12}$$

$$a_{35} = a_{53} = -\frac{1}{2}\cos^2\theta \sum \sin(2\delta_i) \tag{18.13}$$

$$a_{44} = N\cos^2\theta = a_{11}\cos^2\theta \tag{18.14}$$

$$a_{45} = a_{54} = -\frac{1}{2}\sin(2\theta)\sum_i^N \cos\delta_i = -\frac{1}{2}\sin(2\theta) a_{13} \tag{18.15}$$

$$a_{55} = N - \cos^2\theta \sum \cos^2\delta_i = N(1+\sin^2\theta) - a_{33} \tag{18.16}$$

$$b_1 = \sum_i^N V_{Ei}{}^* \tag{18.17}$$

$$b_2 = -\sum_i^N V_{Ei}^* \cos\alpha_i \cos\gamma_i + \cos\theta \sum_i^N V_{Ni}^* \sin\alpha_i + \sin\theta \sum{}_i V_{Ni}{}^* \cos\alpha_i \sin\gamma_i \tag{18.18}$$

$$b_3 = \sum_i^N V_{Ei}{}^* \cos\delta_i - \sin\theta \sum V_{Ni}^* \sin\delta_i \tag{18.19}$$

$$b_4 = \cos\theta \sum_i^N V_{Ni}{}^* \tag{18.20}$$

$$b_5 = -\sum_i^N V_{Ei}^* \sin\delta_i - \sin\theta \sum_i^N V_{Ni}^* \cos\delta_i \tag{18.21}$$

The coefficients in Eqs. (18.1) through (18.21) are calculated with Excell application, while Eq (17) is solved to yield v_s, v_o, v_{x0}, v_{y0} and v_{z0}.

6. Results

Figure 8 shows a typical plot of the laser beam position on the linear array detector versus the 16 angular positions, which are evenly distributed over 360° with an angular accuracy of 0.5°. The position 0 is not exactly pointing south, but at an angle of 9° east of south, while position 15 is 13.5° west of south.

The velocities v_s, v_o, v_x, v_y, and v_z are determined as described in section 5 to be:

$$\begin{cases} v_s = 0.051 \pm 0.94(km/s) \\ v_o = -0.19 \pm 0.94(km/s) \\ v_x = 0.047 \pm 0.94(km/s) \\ v_y = -0.29 \pm 0.94(km/s) \\ v_z = 0.066 \pm 0.94(km/s) \\ v_{drift} = 0.30 \pm 0.94(km/s) \end{cases} \tag{19}$$

where $$v_{drift} = \sqrt{v_x^{\,2} + v_y^{\,2} + v_z^{\,2}} \tag{20}$$

is the ether drift velocity of the solar system at noon on the Summer solstice (June 22) of 2007. The error reported in Eq (19) is σ. The result says that all the velocities obtained are good zeros well within σ. As defined in Eq (15), σ measures the statistical error of the experimental ether drift velocities. Eq(19) shows that the spin velocity of the earth with respect to the ether is zero within 6% of σ; the orbital velocity of the earth with respect to the ether is zero within 20% of σ; and the drift velocity of the solar system with respect to the ether is zero within 32% of σ. These null results are more evident when Eq(19) is compared to the kinetic velocities of the earth given by Eqs(3) and (4):

$$v_s^* = 0.38 km/s$$
$$v_0^* = 29.8 km/s$$

Note that v_s^*=0.38 *km/s* is significantly smaller than our reported experimental error σ, which means that the velocity due to Earth's rotation defies detection unless the data points increases by at least a factor of 6. The comparison shows that the experimental spin velocity of the earth with respect to the ether is only 14% of the kinetic spin velocity of the earth, while the orbital velocity of the earth with respect to the ether is merely 0.6% of the kinetic velocity of the earth, and the ether drift velocity of the solar system, v_{drift} given in Eq(19), is less that 0.15% of the kinetic velocity of the solar system orbiting the galactic center, which is about 200 *km/s*.

7. Conclusion and discussion

We have conducted a first-order ether drift experiment over a period of two years. The data have shown an unquestionable null result. The rotational velocity and orbital velocity of the

earth, and the galactic orbital velocity of the solar system are measured to be, respectively, 0.051 *km/s*, -0.19 *km/s*, and 0.30 *km/s*, which are good zeros well within the statistical error of 0.94 *km/*s. These velocities are merely 14%, 0.6% and 0.15% of the theoretical values of the corresponding kinetic velocities of the earth and the solar system. The percentages might be suggestive of the relative importance of the corresponding movements in ether drift, if such does exist at all.

Our experiment is fundamentally different in principle from the traditional ether drift experiments based on the interference of light. It is free of the fringe-running problem during rotation of the interferometer, and therefore contributes a truly independent experiment from the interference experiments.

Our null result should also be compared to the Roemer Effect of the period of Io orbiting the Jupiter and the Doppler Effect of the spectral lines from the stars. Both of these effects show the positive ether drift effect to the first order with good accuracy. The difference rests on the basic fact that our experiment is a Type II experiment in which there is no relative motion between the source and the detector, while the Roemer Effect and the Doppler Effect experiments are the Type I experiments in which the relative motion between the source (Jupiter or the stars) and the detectors sitting on the Earth do exist. The null results of our experiment and other Type II experiments can be naturally explained if the ether is a medium moving and rotating with the solar system. Such theory provides a classical explanation consistent with the results of our experiment, the star aberration, the Roemer Effect and the Doppler Effect.

It must be noted that our null result with respect to Earth's rotation is subject to doubt because the experimental error is greater than the kinetic linear velocity of the equipment due to Earth's rotation. To establish the "null result" with respect to Earth's rotation beyond doubt, the experimental error needs to be further reduced, either by employing more stable laser, or by increasing the data points. If in a latter improved experiment the ether drift velocity due to Earth's rotation turns out positive, we will be compelled to conclude that the ether is a space medium associated and rotating with the solar system, but not rotating with the Earth. This scenario would in consistent with the operation of the GPS in an Earth-Centered Inertial frame and the measurement by Gift of light speed anisotropy resulting from the Earth's rotation [15].

We also noticed that Sato [16] recently found that the ether may have to be restricted to being associated with the Earth but not extended to the solar system. Such a theory seems inconsistent with the Roemer Effect and the Doppler Effect. However, the inconsistency is not absolutely insolvent. A speculative theory of light propagating with the dominant medium of the highest optical density will resolve such discrepancy. For instance, the air dominates the light propagation within the atmosphere, while the interplanetary medium dominates the light propagation within the solar system, and so on. There is no reason, theoretical or experimental, to assume that the ether, or the space medium, would have the same density on the earth and in the space. After all, the ether may be just the medium present in the space of concern, made of the particles we already know, instead of some mysterious unknown stuff. Such theory of light propagation dominated by the medium with highest optical density remains speculative until more direct evidence become available.

References

[1] A.A. Michelson, Am. J. Sci., **122**, 120 (1881).
[2] A.A. Michelson and E.W. Morley, Am. J. Sci., **134**, 333 (1887).
[3] For a review, see, for example, Shankland, McCuskey, Leone, and Kuerti, Rev. Mod. Phys., **27**, 167 (1955).
[4] E. *A.* Whitaker, *History of the Theories of Aether and Electricity*, (Humanities Press, 1973).
[5] S. Skinner, *Relativity for Scientists and Engineers*, (Dover Publications, 1982).
[6] S.J.G. Gift, *The Relative Motion of the Earth and the Ether Detected*, Journal of Scientific Exploration, **20**, pp201-214 (2006)..
[7] M. Zelik, & E. Smith, *Introductory Astronomy and Astrophysics*, (2nd ed.), p44, (Saunders College Publishing,1987).
[8] For a review of Mascart's experimental work and Potier and Veltmann's theoretical work, see the review by R. Newburgh, *Fresnel drag and the principle of relativity*, Chicago Journals, **65**, No. 3, pp379-386 (1974), (The University of Chicago Press on behave of The History of Science and Society, 1974), and the references thereof.
[9] R.T. Cahill, *Relativity, Gravitation, Cosmology*, (Nova Science Pub., NY, 2004), pp168-226.
[10] R.T. Cahill, *Absolute motion and gravitational effects*, Apeiron, **11**, No.1, pp53-111 (2004).
[11] R.T. Cahill, *Process Physics: from information theory to quantum space and matter*, (Nova Science Pub., NY, 2005).
[12] R.T. Cahill, *The Michelson and Morley 1887 Experiment and the Discovery of Absolute Motion*, Progress in Physics, **3**, pp25-29 (2005).
[13] D.C. Miller, Rev. Mod. Physi., **5**, pp203-242 (1933).
[14] D.G. Torr and P. Kolen, *Precision Measurements and Fundamental Constants*, ed. by B.N. Taylor and W.D. Phillips, Nat. Bur. Stand. (U.S.), Spec. Pub., **617**, 675 (1984).
[15] S.J.G. Gift, Physics Essays, **23**, 2, pp271-275 (2010).
[16] Sato, M, Physics Essays, **23**, 1, pp127-136 (2010).

Captions to the Figures

Figure 1. Experimental Set-up

Figure 2. The shift of laser beam at the linear array detector

Figure 3. Orbital velocity at point A

Figure 4. Transformation of the orbital velocity of the earth from point A to point B

Figure 5. Transformation of the orbital velocity of the earth from point B to point O

Figure 6. The ether drift velocity related to the motion of the solar system.

Figure 7. Transformation of the drift velocity of the solar system from point B to point O

Figure 8. A typical laser beam profile and the Gaussian fit by KaleidaGraph. The correlation is typically 0.997. The standard deviation of the central position is

0.27 channels, corresponding to a distance of 1.8 μm. This central position is used to calculate the shift of laser position.

Figure 9. A photograph of the experimental set-up and the circular pond. The total weight of the steel pipe and the houseboat is estimated to be 3 tons from the measurements of the boat and the draft. One end of the house boat is pivoted at the center of the pond to allow rotational movement. A diode Laser is mounted on the end of the steel pipe near the center of the pond. The linear array detector is mounted on the opposite end of the steel pipe. The boat can be stopped by at 16 positions equally spaced over the full circle by a steel pin. The stopping pin and the pivoting pin allow the boat to freely float vertically.

Figure 1

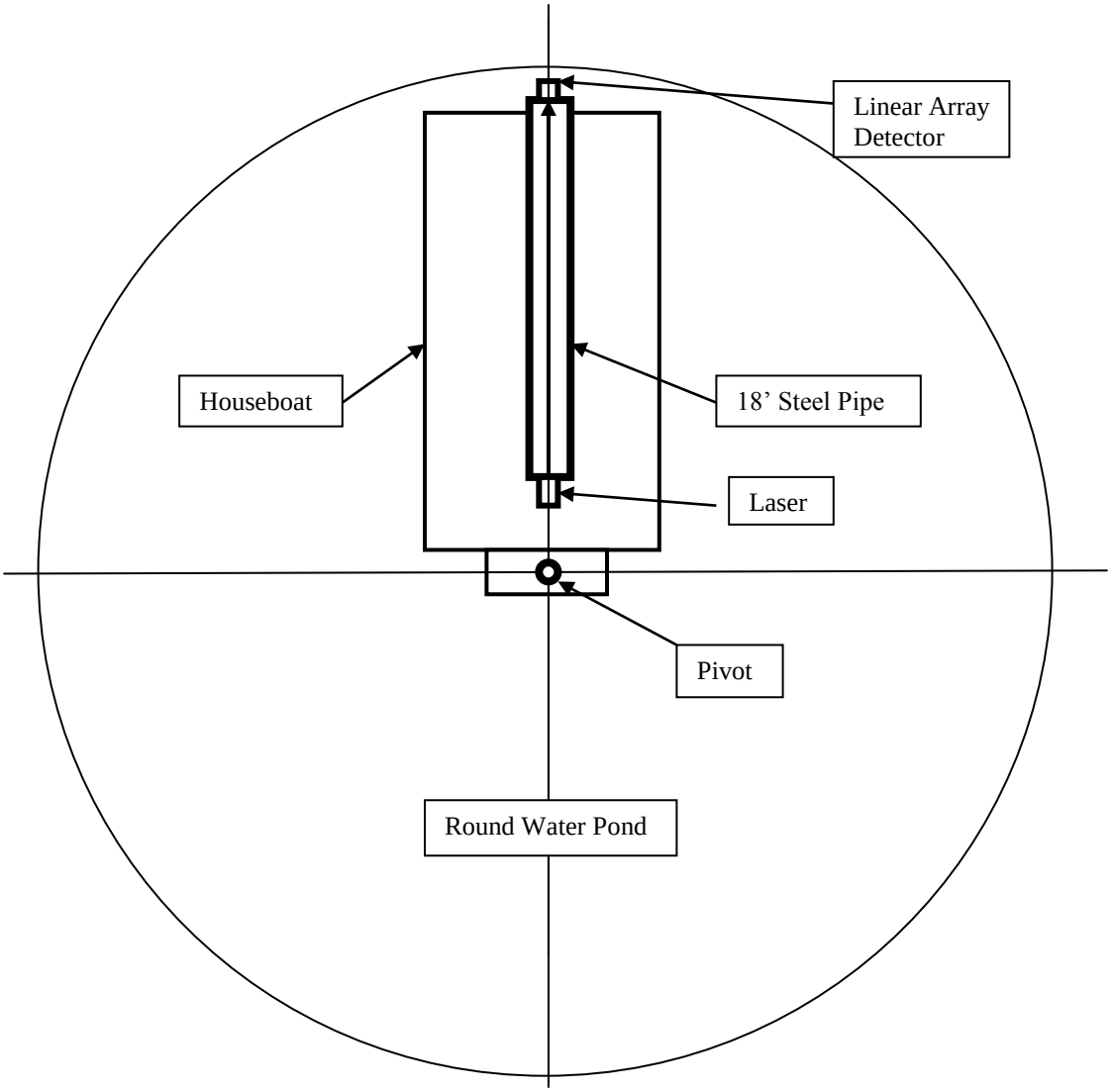
Linear Array Detector
Houseboat
18’ Steel Pipe
Laser
Pivot
Round Water Pond

Figure 2

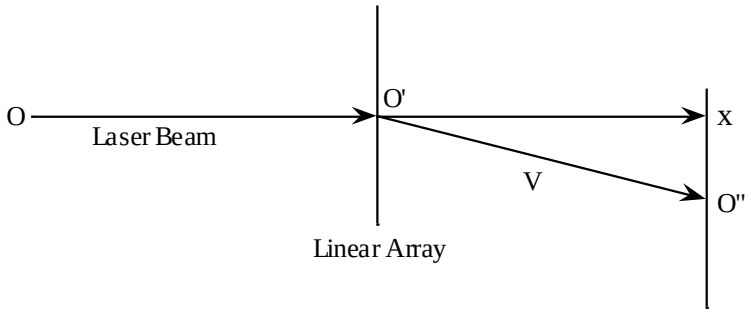

Figure 3. Orbital Velocity at Point A

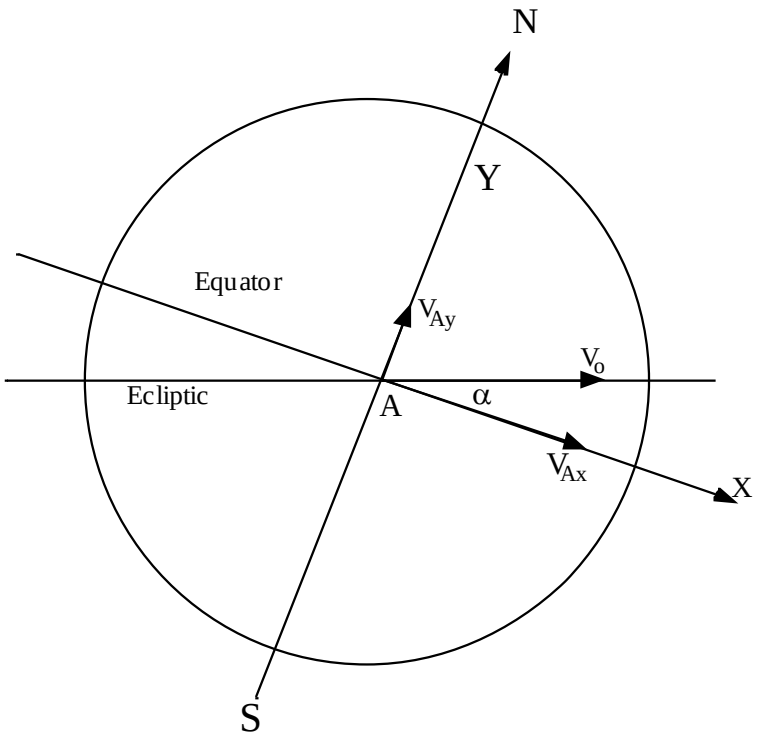

Figure 4. Transformation of Orbital Velocity from Point A to Point B

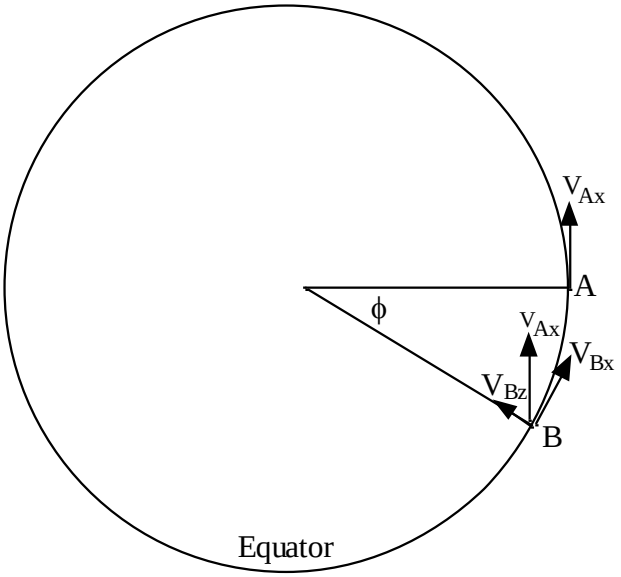

Figure 5. Transformation of Orbital Velocity from Point B to Point O

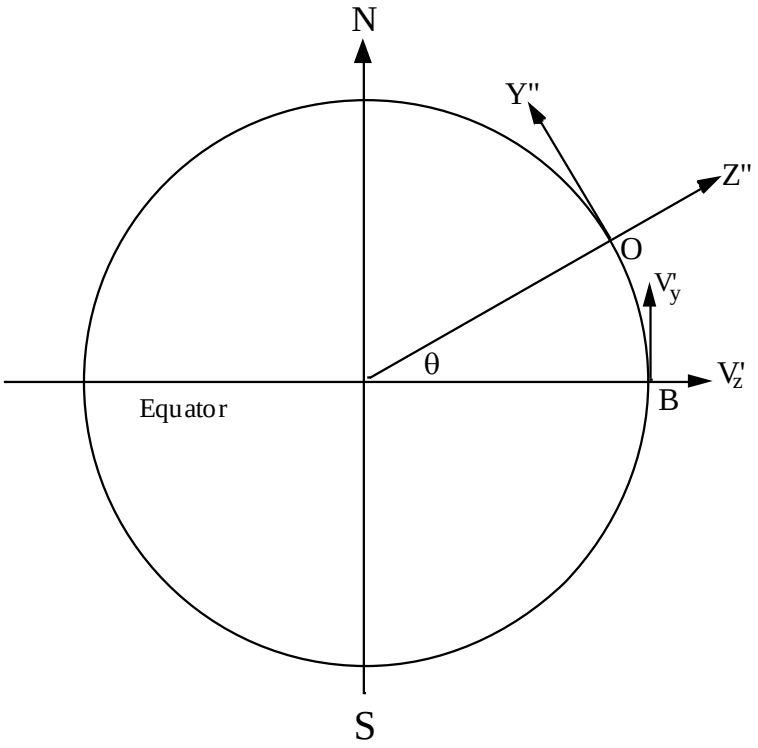

Figure 6. The Drift Velocity With Respect to Ether

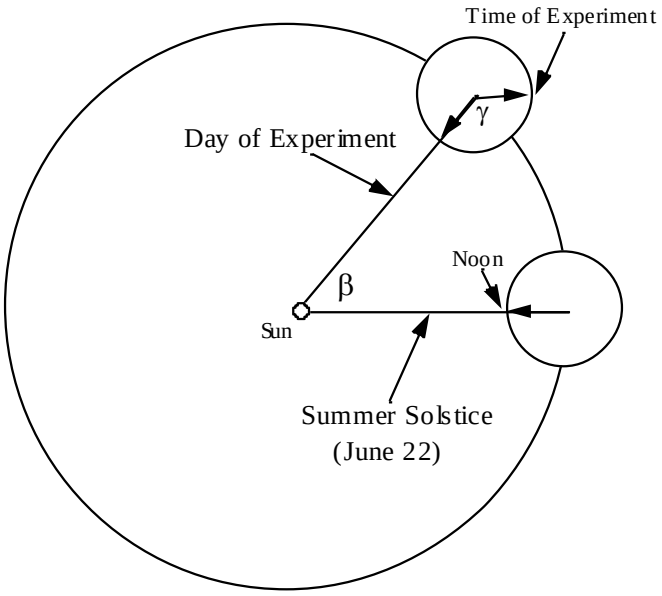

Figure 7

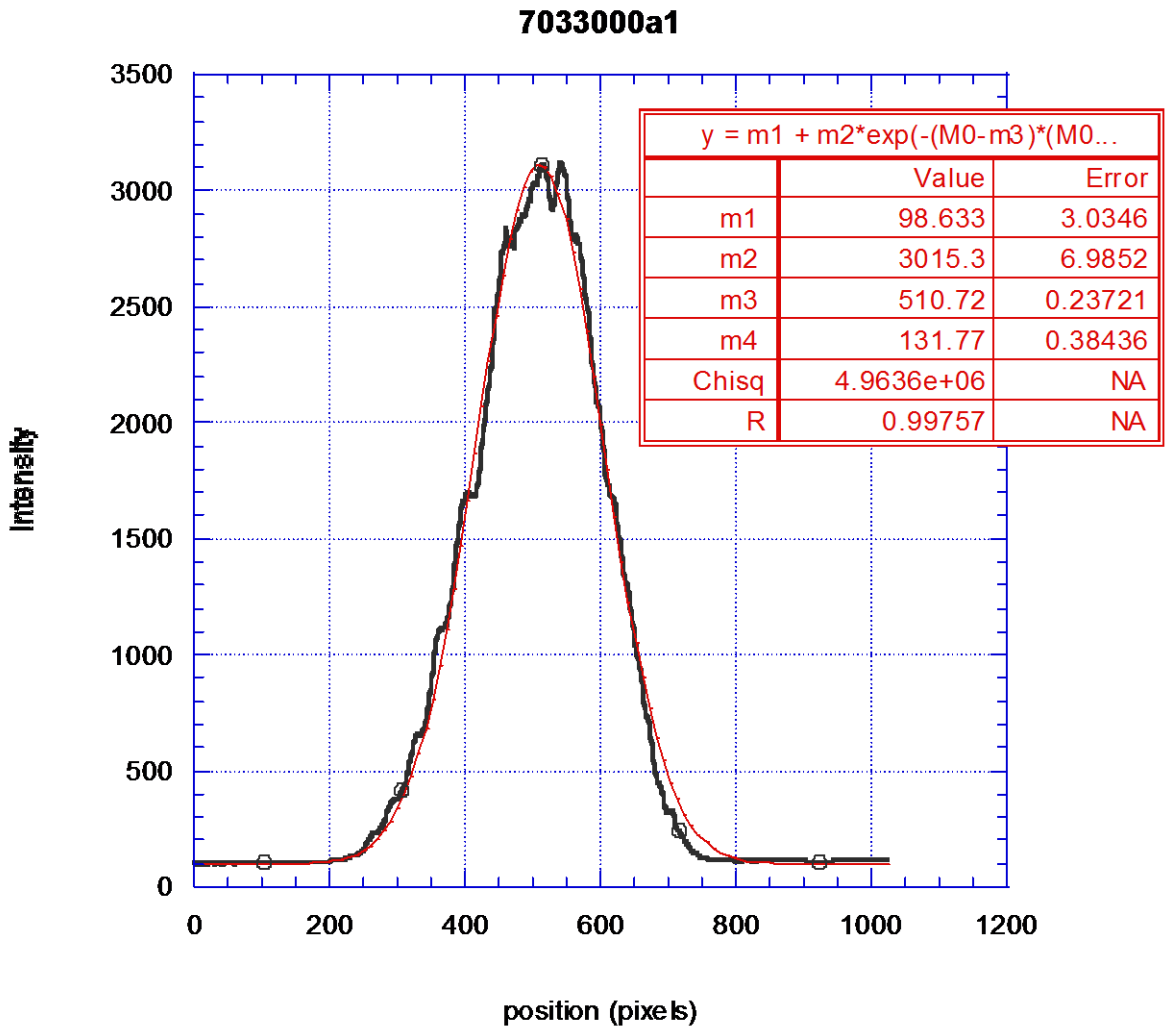
7033000a1
Intensity
position (pixels)
0
500
1000
1500
2000
2500
3000
3500
0
200
400
600
800
1000
1200
y = m1 + m2*exp(-(M0-m3)*(M0...
Value
Error
m1
98.633
3.0346
m2
3015.3
6.9852
m3
510.72
0.23721
m4
131.77
0.38436
Chisq
4.9636e+06
NA
R
0.99757
NA

Figure 8

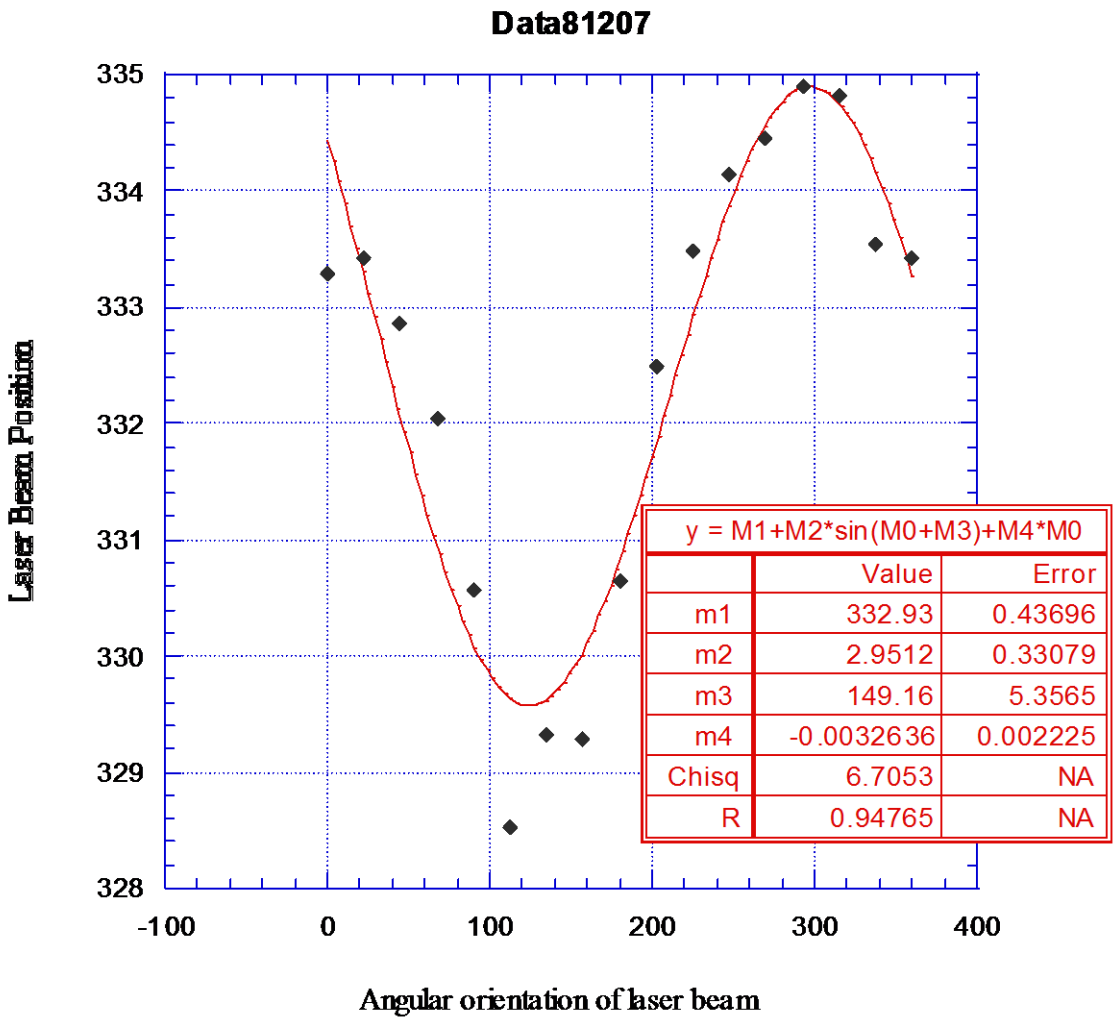
Data81207
335
334
333
332
331
330
329
328
-100
0
100
200
300
400
Laser Beam Position
Angular orientation of laser beam
y = M1+M2*sin(M0+M3)+M4*M0
Value
Error
m1
332.93
0.43696
m2
2.9512
0.33079
m3
149.16
5.3565
m4
-0.0032636
0.002225
Chisq
6.7053
NA
R
0.94765
NA

Figure 9